# Supporting information

## High-performance supercapacitors based on hierarchically porous carbons with a three-dimensional conductive network structure

Jizhao Zou,[a] Wenxuan Tu,[a] Shao-Zhong Zeng,[a] Yuechao Yao,[a] Qi Zhang,[b] Hongliang Wu,[a] Tongbin Lan,[a] Shiyu Liu [a] and Xierong Zeng [a, c, *]

[a] Shenzhen Key Laboratory of Special Functional Materials & Shenzhen Engineering Laboratory for Advance Technology of Ceramics, College of Materials Science and Engineering, Shenzhen University, Shenzhen 518060, P. R. China.

[b] School of Aerospace, Transport and Manufacturing, Cranfield University, Cranfield, Bedfordshire, MK43 OAL, UK.

[c] Guangdong JANUS Intelligent Group Corporation Limited, Dongguan 441900, China.

* Corresponding author.

E-mail address: zengxier@szu.edu.cn (X. R. Zeng)

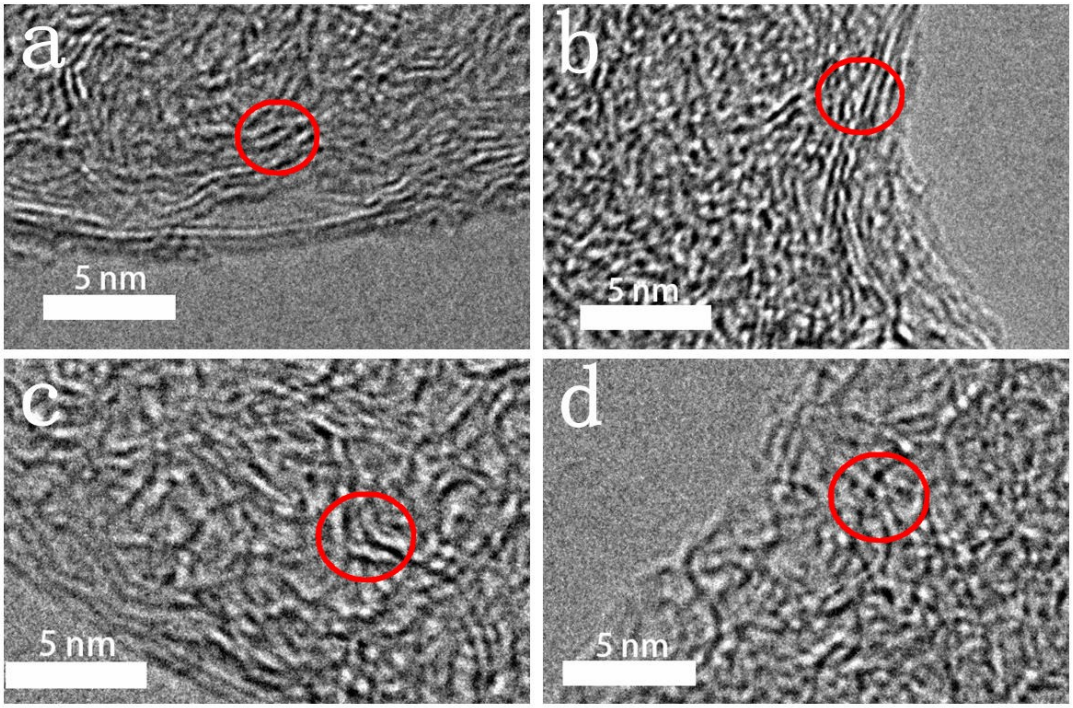


**Fig. S1.** HRTEM images of (a) CsCNBs*3, (b) CsCNBs*4, (c) CsCNBs*5, (d) CsCNBs-950-40.

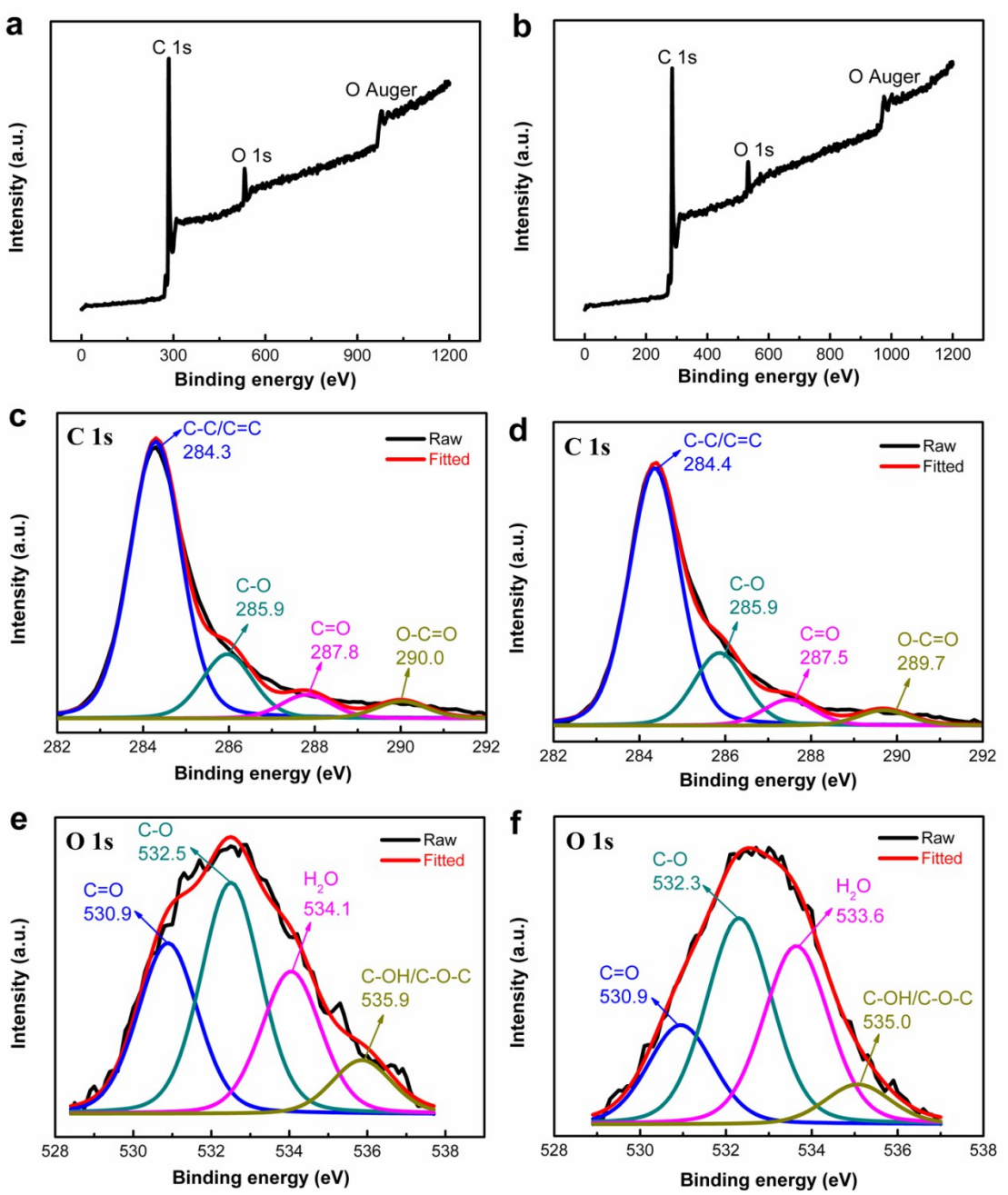


**Fig. S2.** XPS results of the CsCNBs*3 sample: (a) XPS survey, (c) C 1s spectrum, and (e) O 1s spectrum; XPS results of the CsCNBs*5 sample: (b) XPS survey, (d) C 1s spectrum, and (f) O 1s spectrum.

**Table S**1

Physical properties of activated carbon materials.

| Sample | Elemental analysis | | | XPS | |
|---|---|---|---|---|---|
| | C (%) | H (%) | O (%) | C (%) | O (%) |
| CsCNBs*3 | 89.91 | 0.36 | 9.73 | 92.87 | 7.13 |

| | | | | | |
|---|---|---|---|---|---|
| CsCNBs*4 | 90.01 | 0.31 | 9.68 | 92.78 | 7.22 |
| CsCNBs*5 | 93.05 | 0.36 | 6.59 | 93.17 | 6.83 |
| CsCNBs-950-40 | 94.61 | 0.11 | 5.28 | 96.54 | 3.46 |

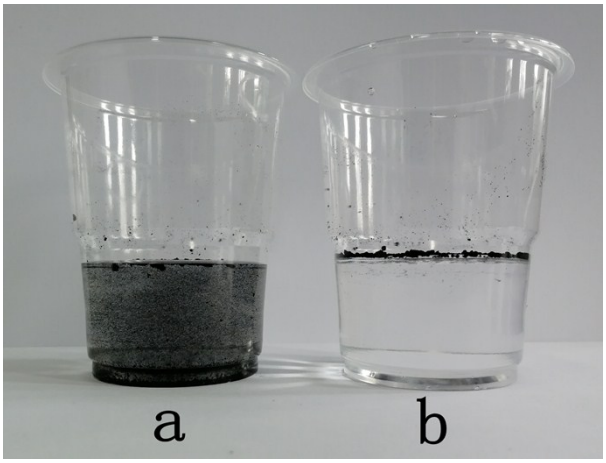


**Fig. S3.** Digital photograph of a simple hydrophilic test of (a) CsCNBs*4 and (b) CsCNBs-950-40, respectively.

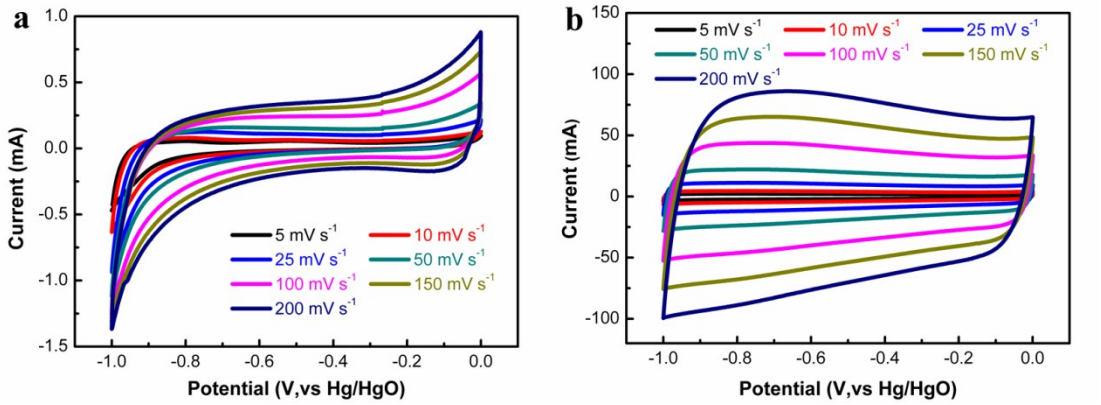


**Fig. S4.** CV curves of (a) a bare foamed nickel electrode and (b) a loaded (CsCNBs*4) electrode at various scan rates ranging from 5 to 200 mV $s^{-1}$.

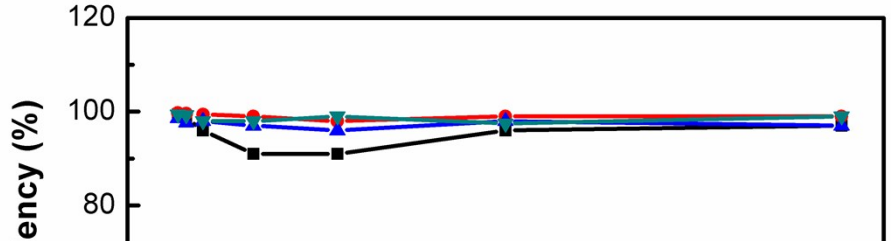

**Fig. S5.** Coulombic efficiencies of four samples measured in a three-electrode system using 6 M KOH electrolyte.

The CsCNBs material before KOH activation is named as CsCNBs-800. Fig. S6a shows the CV curves of the CsCNBs-800 electrode obtained at various scanning rates from 5 to 200 mV $s^{-1}$. All of the CV profiles exhibit symmetric and nearly rectangular shapes, implying its good charge storage ability. The corresponding specific capacitances are caculated by Eq. (1) in Fig. S6b. The CsCNBs-800 electrode displays a high specific capacitance of 155.7 F $g^{-1}$ and specific capacitance retention ratio of 74.5% at 100 mV $s^{-1}$. Fig. S6c shows the GCD curves of CsCNBs-800 electrode at current densities from 0.5 to 40 A $g^{-1}$. The symmetrical isosceles triangular GCD curves indicative the high reversible and ideal supercapacitor behaviour. The corresponding specific capacitances were caculated by Eq. (2) in Fig. S6d. The CsCNBs-800 electrode displays a high specific capacitance of 156 F $g^{-1}$ at 0.5 A $g^{-1}$. In Fig. S6e, the coulombic efficiencies are close to 100%, indicating efficient charge-discharge efficiency. Fig. S6f shows the Nyquist plot and fitting Nyquist plot of CsCNBs-800 electrode in the frequency range from 0.01 Hz to 100 kHz. The resistances (Rs) and charge transfer resistances (Rct) of sample CsCNBs-800 are 0.84 Ω and 0.38 Ω, respectively. It can be seen from Figure 5 that the materials after KOH activation have superior capacitance performance, compared with sample CsCNBs-

800. To sum up, the KOH activation can greatly increase the specific capacity and conductivity of CsCNBs materials.

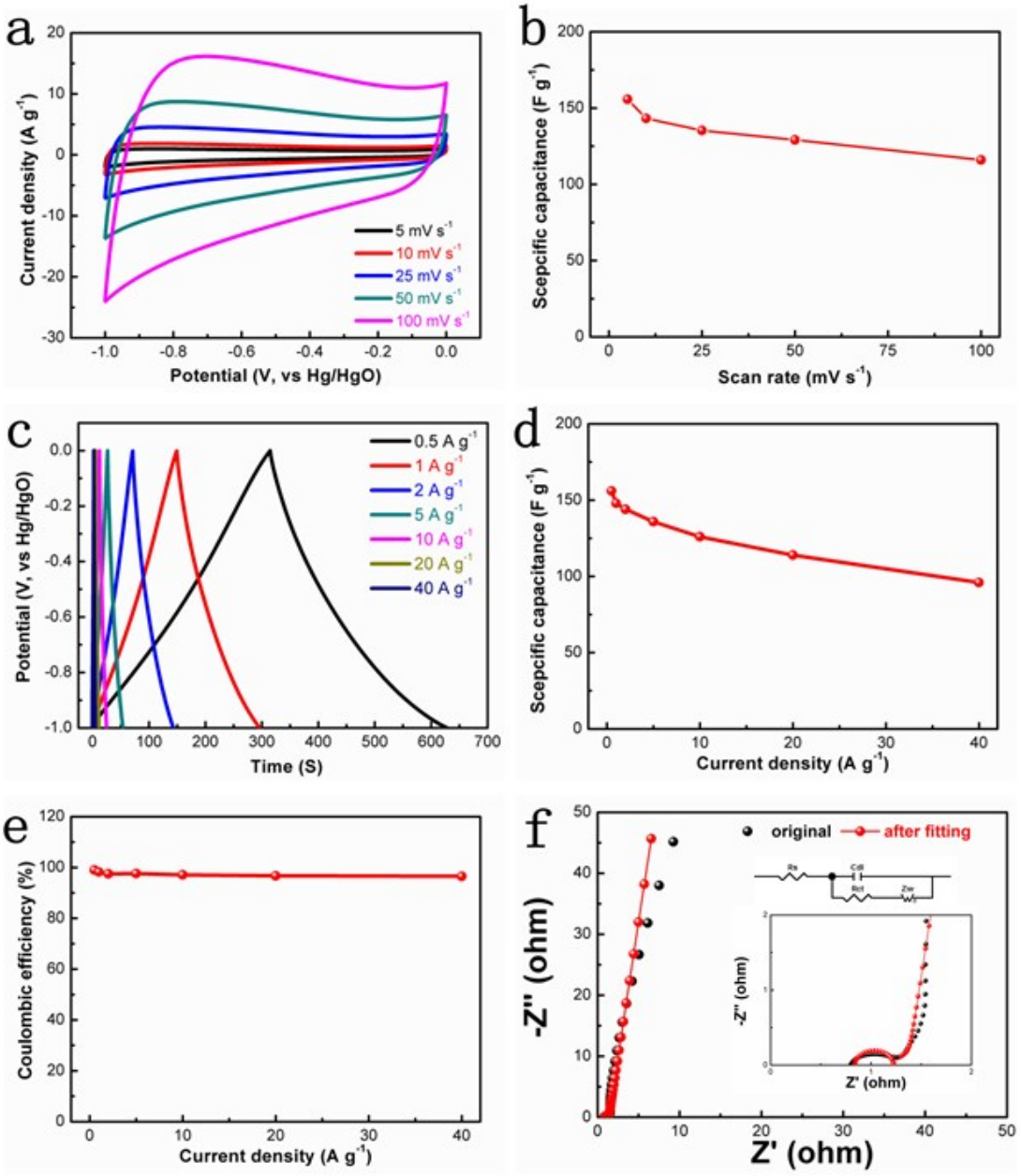


**Fig. S6.** CsCNBs-800: (a) CV curves at various scanning rates ranging from 5 to 200 mV $s^{-1}$; (b) specific capacitances at various potential scanning rates; (c) GCD curves at different current densities ranging from 0.5 A $g^{-1}$ to 40 A $g^{-1}$; (d) specific capacitances at various current densities; (e) the curve of coulombic efficiency; (f) Nyquist plot and fitting Nyquist plot measured in a three-electrode system using 6 M KOH electrolyte. The inset shows the enlarged view of the high-frequency region and the electrical equivalent circuit for fitting impedance spectra.

**Table S2**

The fitting parameters of fitting Nyquist plots of the five electrodes in a three-electrode system using 6 M KOH as the electrolyte.

| sample | Rs (Ω) | Cdl (F) | Rct (Ω) | Zw-R (Ω) | Zw-T (Ω) | Zw-P (Ω) |
|---|---|---|---|---|---|---|
| CsCNBs-800 | 0.84 | 0.001 | 0.38 | 0.64 | 0.16 | 0.46 |
| CsCNBs*3 | 0.56 | 0.001 | 0.27 | 0.61 | 0.11 | 0.48 |
| CsCNBs*4 | 0.22 | 0.0006 | 0.26 | 0.52 | 0.17 | 0.48 |
| CsCNBs*5 | 0.52 | 0.0009 | 0.51 | 0.51 | 0.08 | 0.48 |
| CsCNBs-950-40 | 0.53 | 0.0009 | 0.57 | 0.93 | 0.08 | 0.47 |

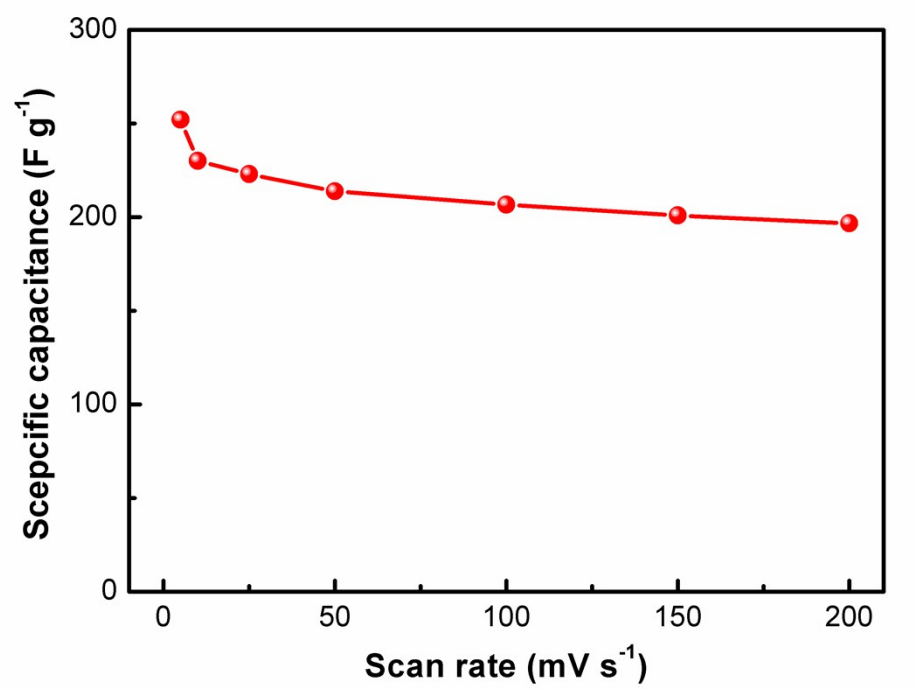


**Fig. S7.** The specific capacitances of sample CsCNBs*4 at various potential scanning rates in a two-electrode system using 6 M KOH electrolyte.

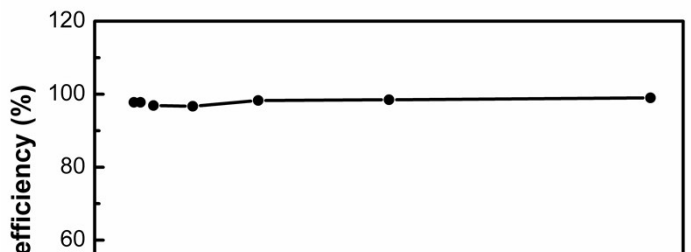

**Fig. S8.** Coulombic efficiency of sample CsCNBs*4 measured in a two-electrode system using 6 M KOH electrolyte.

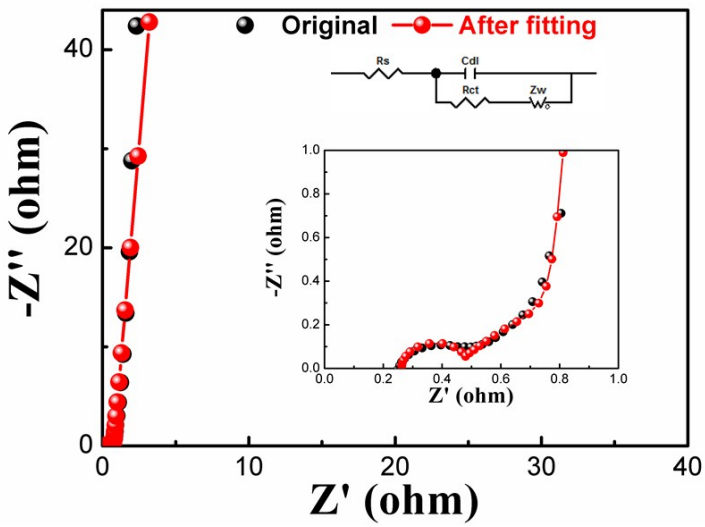


**Fig. S9.** The Nyquist plot and fitting Nyquist plot of the CsCNBs*4 measured in a two-electrode system using 6 M KOH electrolyte. The inset shows the enlarged view of the high-frequency region and the electrical equivalent circuit for fitting impedance spectra.

**Table S3**

The fitting parameters of fitting Nyquist plots of CsCNBs*4 electrode in a two-electrode system using 6 M KOH as the electrolyte.

| sample | Rs (Ω) | Cdl (F) | Rct (Ω) | Zw-R (Ω) | Zw-T (Ω) | Zw-P (Ω) |
|---|---|---|---|---|---|---|
| CsCNBs*4 | 0.26 | 0.0006 | 0.23 | 1.01 | 0.10 | 0.48 |

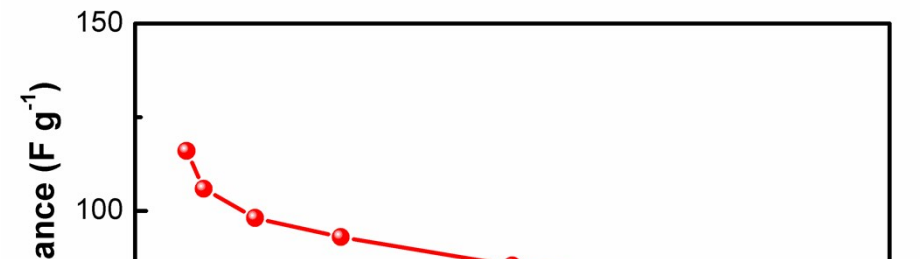

**Fig. S10.** The specific capacitances of sample CsCNBs*4 at various potential scanning rates in a two-electrode system using 1 M $TEABF_4$/AN electrolyte.

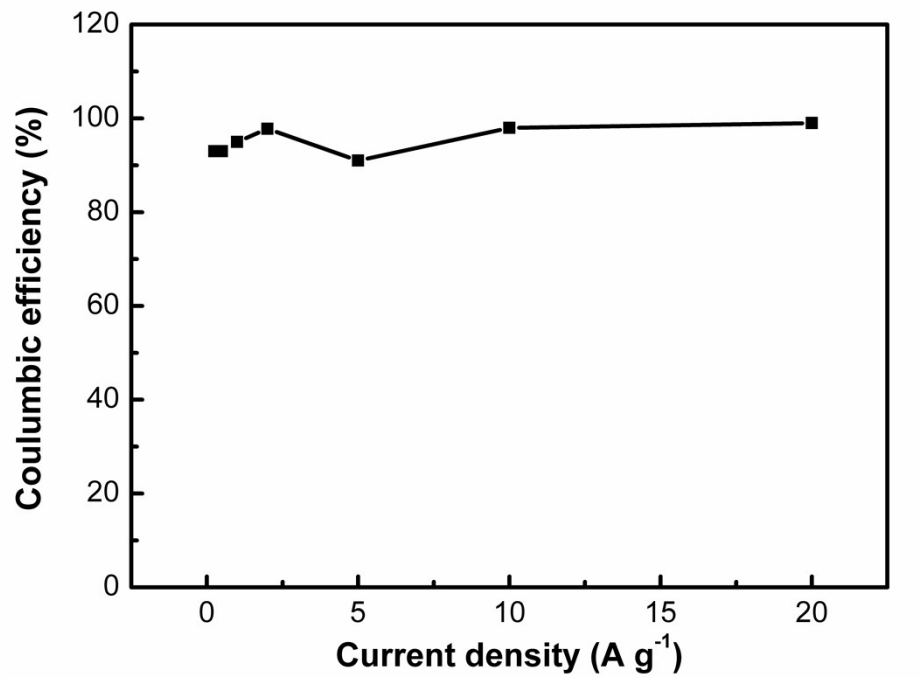


**Fig. S11.** Coulombic efficiency of sample CsCNBs*4 measured in a two-electrode system using 1 M $TEABF_4$/AN electrolyte.

**Table S4**

The fitting parameters of fitting Nyquist plots of the five electrodes in a three-electrode system using 6 M KOH as the electrolyte.

| sample CsCNBs*4 | Rs (Ω) | Cdl (F) | Rct (Ω) | Zw-R (Ω) | Zw-T (Ω) | Zw-P (Ω) |
|---|---|---|---|---|---|---|
| befor cycling | 2.0 | 0.000015 | 1.0 | 0.98 | 0.13 | 0.48 |
| after 15000 cycles | 2.4 | 0.000008 | 1.8 | 250 | 88 | 0.67 |